Journal of Organometallic Chemistry 758 (2014) 19–24

Contents lists available at ScienceDirect

Journal of Organometallic Chemistry

journal homepage: www.elsevier.com/locate/jorganchem

A novel macrocyclic organotin carboxylate containing a penta-nuclear long ladder

Aboubacar Sidiki Sougoule [a], Zemin Mei [b], Xiao Xiao [a], Cheick Abdoul Balde [c], Salematou Samoura [c], Arouna Dolo [a], Dongsheng Zhu [a,*]

[a] Department of Chemistry, Northeast Normal University, Changchun 130024, China
[b] Department of Chemistry, Baicheng Normal University, Baicheng 137000, China
[c] Department of Chemistry, University of Conakry, Guinea

ARTICLE INFO

Article history:
Received 7 December 2013
Received in revised form
5 January 2014
Accepted 17 January 2014

Keywords:
Organotin (IV) compound
Synthesis
Crystal structure
Antitumor activity

ABSTRACT

A novel macrocyclic organotin carboxylate [(n-$Bu_2SnO)_5L$] (complex **1**) [H_2L = (3-carboxymethoxyphenoxy) acetic acid] was synthesized by the reaction of di-n-butyltin oxide with H_2L and is characterized by elemental analyses i.e. IR ^{1}H NMR and UV spectroscopies. X-ray crystallography diffraction analysis reveals that complex **1** is a centrosymmetric macrocycle and contains a penta-nuclear four-fold-ladder-like organo-oxotin cluster. All five Sn atoms are five-coordinated and the coordination environment can be considered as a trigonal bipyramidal. The luminescent property of complex **1** has also been investigated. Pilot studies have confirmed that complex **1** has shown good antitumor activity.

1. Introduction

In the recent years, the interests in organotin (IV) compounds $R_nSnX_{(4-n)}$ ($n = 1–4$) are increasing because of their biological activity, reactivity, and industrial applications [1–6]. In the last few decades, some structures of organotin (IV) carboxylates are well recognized and a wide variety of coordination geometries have been reported [7–9]. However, at the same time new applications of such compounds are being discovered in industry, ecology, and medicine. Recently, much attention has also been focused on their use as metal-based drugs [4]. In general, the biochemical activity of organotin (IV) compounds is mainly determined by the structure of the molecule and the coordination number of the tin atoms [10–17]. The latter aspect has been actively investigated by a large number of researchers, and a multitude of structure types including monomers, dimers, tetramers, oligomeric ladders and hexameric drums are discovered [18]. For the ladder-like structure, as far as we research, centrosymmetric ring with double ladders bridged by two ligands are more common in reported literatures [19–21]. The only single-ladder macrocycle organotin containing longest ladder bridged by one ligand was synthesized by our group [22].

As the continue study of ladder-like structure in organotin chemistry, we projected to synthesize another “single-ladder”. In the present study, a flexible dicarboxylic acid H_2L as ligand has been chosen. Because H_2L is interesting because of the following reasons: (a) strong coordination tendency with Sn and rich coordination modes; (b) helping to form 2D and 3D moderately robust networks; (c) here long molecular lengths tending to construct a special macrocycle. Herein we report the synthesis, characterization, antitumor activity and luminescent properties of complex **1**. Complex **1** has been prepared by azeotropic removal of H_2O from the reaction of the di-n-butyltin oxide with H_2L in the solvent mixture of toluene and ethanol. It is a 16-membered unusual macrocycle with a single-ladder and the organotin carboxylate containing one penta-nuclear four-fold-ladder-like organo-oxotin unit. The preliminary fluorescent properties and antitumor activity have also been investigated. This is likely to serve as a new model for further study on the fluorescent properties and biological activity of complex **1**.

2. Experimental

2.1. General and instrumental

The reagents and solvents were purchased as supplied and used without further purification. Melting point was determined with digital melting point apparatus. Elemental analyses were carried

* Corresponding author. Tel.: +86 13009010567; fax: +86 0431 85684009.
E-mail address: zhuds206@nenu.edu.cn (D. Zhu).

http://dx.doi.org/10.1016/j.jorganchem.2014.01.034
0022-328X/

out on a Perkin–Elmer PE 2400 CHN instrument and gravimetric analysis for Sn. ^{1}H NMR spectra were recorded in $CDCl_3$ on a Varian Mercury 300 MHz spectrometer. Infrared spectra (KBr pellets) were recorded on an Alpha Centauri FI/IR spectrometer (400–4000 cm^{-1} range). The UV–vis absorption spectrum was recorded by a Varian Cary 500i UV–vis–NIR spectrophotometer. The luminescent properties of the ligand and complex were measured on a Perkin–Elmer FLS-920 spectrometer.

2.2. X-ray crystallography

Crystals of complex **1** was grown by slow evaporation of a mixture toluene/ethanol (10:1, 50 mL) solution at room temperature. The colorless crystals were mounted on a sealed tube and used for data collection. Single-crystal X-ray diffraction data for the complex were recorded on a Bruker CCD Area Detector diffractometer by using the ω/φ scan technique with Mo-kα radiation ($\lambda = 0.71073$ Å). Absorption corrections were applied by using multiscan techniques [23]. The structures were solved by direct methods with SHELXS-97 [24] and refined by full-matrix least squares with SHELXL-97 [25] within WINGX [26]. All nonhydrogen atoms were refined with anisotropic temperature parameters and hydrogen atoms were refined as rigid groups. A summary of the crystal data, experimental details and refinement results are listed in Table 1.

2.3. Synthesis

2.3.1. Synthesis of (3-carboxymethoxy-phenoxy) acetic acid (H_2L)

11.0 g (0.1 mol) of resorcinol, 200 mL of water and 20.0 g (0.5 mol) of solid sodium hydroxide were added into the three-necked flask. Mixed them till dissolved. Then 21.0 g (0.22 mol) of monochloroacetic acetic was added. The mixture was stirred for 4 h and heated between 95 and 100 °C. After cooling to the room temperature, it was acidified with 4 mol/L of hydrochloric acid till pH = 2–3. Then a large number of solid precipitated. The solid crude product was dissolved into the water (100 mL) and the excess solvent was removed by filtration. Finally the filtrate was acidified with 4 mol/L hydrochloric acid to obtain pH = 2–3 and the solid precipitated. It was washed with water to obtain a pure white powder. The powder was placed in drying oven at 150 °C for 3 h before all the characterizations to remove the water. Yield: 76%, m.p: 191.5–192.0 °C. IR (KBr, cm^{-1}): υ(O–H···O) 3253; υ_{as}(COO) 1761; υ_{sym}(COO) 1433. ^{1}H NMR ($CDCl_3$, ppm): 4.64 (m, 4H, $-CH_2-$), 6.44–7.16 (m, 4H, Ar-H). Anal. Calc. for $C_{10}H_{10}O_6$ (226.18 g/mol): C, 53.11; H, 4.46%. Found: C, 53.07; H, 4.42%.

2.3.2. Synthesis of complex **1**

A solution of (3-carboxymethoxy-phenoxy) acetic acid (H_2L) (0.113 g, 0.5 mmol) and di-*n*-butyltin oxide (0.747 g, 3 mmol) was dissolved in toluene/ethanol (5:1, 50 mL) and refluxed for 20 h using a dean stark funnel. After cooling to room temperature, the solvent mixture was removed by filtration and transparent colorless crystals were obtained. The product was placed in drying oven at 110 °C for 3 h before all the characterizations to remove the solvent. Yield: 63%, m.p: 248.2–249.5 °C. Anal. Calc. for $C_{50}H_{100}O_{11}Sn_5$ (1470.75 g/mol): C, 40.83; H, 6.85%. Found: C, 40.88; H, 6.79%. IR (KBr, cm^{-1}): υ(C–H), 2923, 2871, 2856; υ_{as}(COO) 1607; υ_{sym}(COO) 1396; υ(Sn–O–Sn) 454; υ(Sn–C) 578. ^{1}H NMR ($CDCl_3$, ppm): 0.92 (t, 30H, $J = 6.8$, $-CH_3$), 1.05–1.68 (m, 60H, $SnCH_2CH_2CH_2-$), 4.51 (m, 24H, Ar-CH_2-), 6.35–6.82 (m, 28H, Ar-H) (Scheme 1).

2.4. MTT assay

Hela cell lines were grown in culture media containing 10% NCS, 1% HEPES and 1% RPMI1640 in a 5% CO_2 incubator at 37 °C. The effects of di-*n*-butyltin oxide and complex **1** on cell growth were evaluated using the MTT assay [27]. A total of 2×10^3 cells were seeded in the 96-well plate and cultured for 24 h. Thereafter, the cells were treated with various concentrations of di-*n*-butyltin oxide and complex **1** for 24 h. After exposure to the drug, the MTT assay was carried out. All experiments were performed at least three times and the mean percentage of proliferation was calculated.

3. Results and discussion

3.1. IR spectra

The comparative analysis for the IR spectra of the ligand H_2L and the complex **1** indicates that –OH vibration bands at 3100–3500 cm^{-1} are absent in that of complex **1** spectrum; hence it is evidenced that metal–ligand bond formation has taken place through –COO groups. The υ_{as}(COO) and υ_{sym}(COO) are at 1607 cm^{-1} and 1396 cm^{-1} respectively. The Δ [υ_{as}(COO) − υ_{sym}(COO)] value of complex **1** (211 cm^{-1}) is close to that found in the monodentate [28,29].

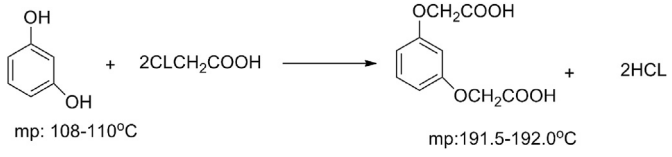

Scheme 1.

Table 1
Crystal data and structure refinement for complex **1**.

Empirical formula	$C_{50}H_{100}O_{11}Sn_5$
Formula weight	1470.75
T (K)	293(2)
Crystal size (mm)	0.21 × 0.16 × 0.14
Wavelength (Å)	0.71073 Å
Crystal system	Monoclinic
Space group	$P2(1)/n$
a (Å)	21.1335(17)
b (Å)	13.3934 (10)
c (Å)	23.4488(18)
α (°)	90
β (°)	106.2250(10)
γ (°)	90
V (Å^3)	6372.8(9)
Z	4
$D_{calc.}$ (mg/m^3)	1.533
Absorption coefficient, μ (mm^{-1})	1.980
F(000)	2952
Scan mode	ω
θ Range for data collection (°)	1.53, 26.05
Reflections collected/unique [$R_{(int)}$]	38,330/12,459 [$R_{(int)} = 0.0220$]
Data/parameters	12,459/45/547
Final R induces [$I > 2\sigma$ (I)]	$R_1 = 0.0477$, $wR_2 = 0.1327$
R induces (all data)	$R_1 = 0.0568$, $wR_2 = 0.1418$
Goodness-of-fit (GOF) on F^2	1.041
Max. and min. transmission	0.7580 and 0.6910
Completeness to $\theta = 25$	99.4%
Absorption correction	Semi-empirical from equivalents
Refinement method	Full-matrix least-squares on F^2

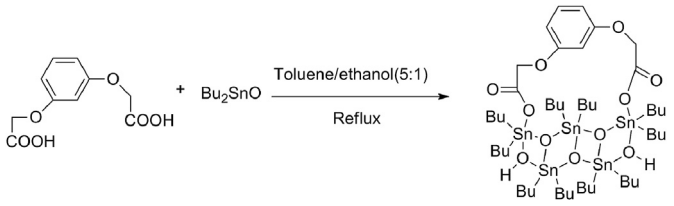

Scheme 2.

3.2. ^{1}H NMR spectra

In the ^{1}H NMR spectrum of ligand, the COOH group resonance appears at 11–12 ppm and disappears when the carboxyl group participates in coordination to the Sn atoms in complex **1**. The NMR spectrum of complex **1** shows that multiple resonance peaks are shown in the range of 1.05–1.68 ppm by the protons of $-CH_2-CH_2-CH_2-$ skeleton while three protons of the terminal methyl groups showed a sharp peak at 0.91 ppm. The chemical shifts of the protons on the phenyl groups of complex **1** exhibit signals at 6.35–6.82 ppm as multiplets, while the protons on methylene groups show resonance at 4.51 ppm (Scheme 2).

3.3. Crystal structure

The molecular structure of complex **1** is shown in Fig. 1 and the selected bond lengths and angles are listed in Table 2. The crystal cell of complex **1** is a 16-membered macrocycle consists of a pentanuclear organo-oxotin skeleton [$Sn_5(\mu_3\text{-}O)_5$] and a ligand H_2L chelated via monodentate coordination mode. O(1), O(2) and O(5) of the skeleton are coordinated with three Bu_2Sn units. Therefore they are three-coordinated and adopt planar trigonal geometry. O(3) and O(5) are bound by two Bu_2Sn units. All Sn atoms in complex **1** are five-coordinated, showing a trigonal bipyramid configuration but having two chemical environments. Sn(3)–Sn(5) are coordinated with three μ_3-O atoms and two C atoms from butyl groups, while the coordinated O atoms O(6) and O(8) for Sn(1) and Sn(2) are from the carboxylate group of ligand H_2L. The C–Sn–C angles are 125.9(5)° and 132.4(6)° for Sn(1) and Sn(2) respectively, much larger than those of Sn(3)–Sn(5) [123.0(3)–123.1(4)°], which are caused by the less space congestion of terminal position in the organooxotin unit. Axial O–Sn–O angles of Sn(1) and Sn(2) [155.99(16) and 155.67(16)°] are larger than those of Sn(4)–Sn(5) [148.32(16)–149.21(17)°] for the same reason. The $Sn_5(\mu_3\text{-}O)_5$ cluster demonstrates that along ladder consists of four twisted $Sn_2(\mu_3\text{-}O)_2$ distannoxane units. Excluding two end units, they are approximate to parallelogram, proved by the Sn–O bond lengths of Sn(4)–Sn(5) range from 2.046(4) to 2.158(4) Å, and the related O–Sn–O [74.20(15)–75.22(14)°] and Sn–O–Sn [104.67(14)–105.38(15)°] angles listed in Table 2. However, the both end units are more twisted with the Sn–O bond lengths of Sn(1) and Sn(2) owing larger span which range from 2.013(3) to 2.185(5) Å. And the torsion is still indicated by the smaller O–Sn–O [74.57–74.58(15)°] and larger Sn–O–Sn (100.85–110.46°) angles. All the bond lengths and angles are in agreement to those of previously synthesized complexes [21,30–32]. "Ladder" $Sn_5(\mu_3\text{-}O)_5$ is almost coplanar and because of the steric hindrance, $Sn_5(\mu_3\text{-}O)_5$ ladder is of zig-zag shape. Ligand H_2L chelates with the organo-oxotin ladder by

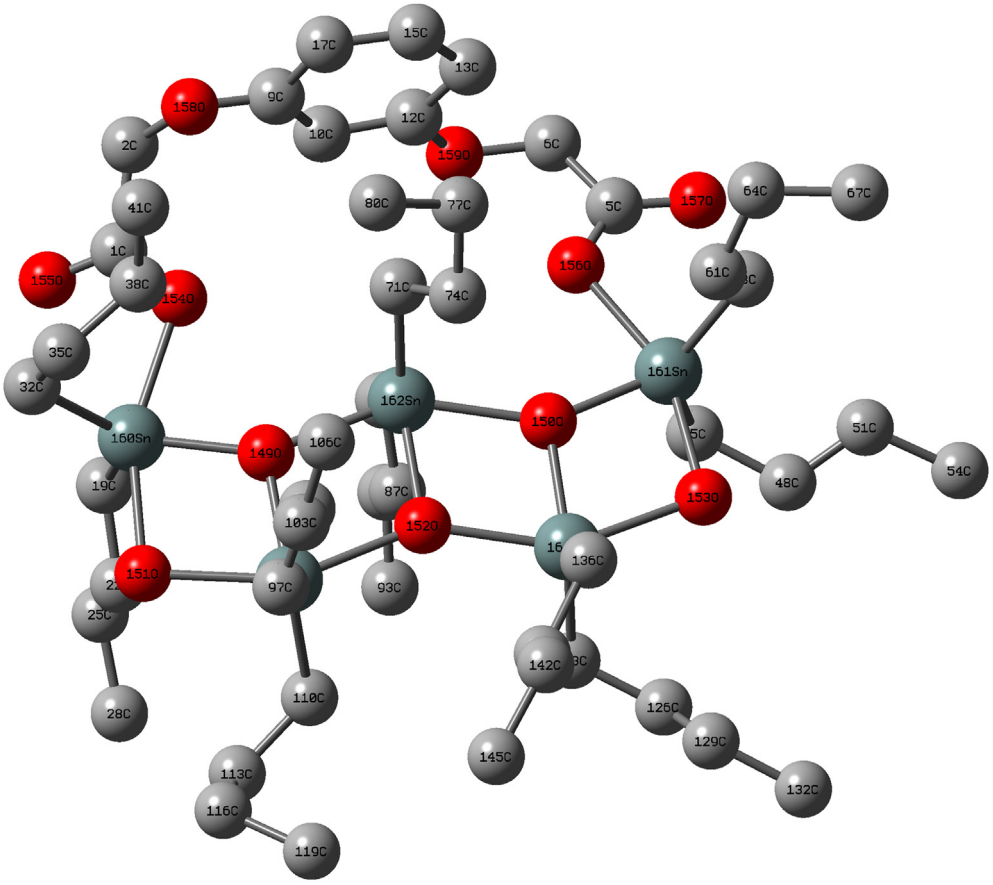

Fig. 1. The molecular structure of complex **1**.

Table 2
Selected bond lengths (Å) and angles (°) for complex **1**.

Bong lengths			
Sn(1)–O(1)	2.013(3)	Sn(4)–C(81)	2.129(6)
Sn(1)–O(6)	2.210(4)	Sn(4)–O(3)	2.155(4)
Sn(1)–O(3)	2.168(5)	Sn(4)–C(71)	2.137(7)
Sn(1)–O(7)	3.062(3)	Sn(4)–O(1)	2.046(4)
Sn(1)–C(11)	2.118(7)	Sn(4)–O(4)	2.119(3)
Sn(1)–C(21)	2.121(14)	Sn(5)–C(101)	2.110(7)
Sn(2)–C(31)	2.139(9)	Sn(5)–O(5)	2.158(4)
Sn(2)–C(41)	2.100(14)	Sn(5)–O(2)	2.037(4)
Sn(2)–O(2)	2.006(3)	Sn(5)–O(4)	2.124(3)
Sn(2)–O(9)	3.108(5)	Sn(5)–C(91)	2.122(7)
Sn(2)–O(8)	2.185(5)	C(3)–O(8)	1.264(8)
Sn(2)–O(5)	2.159(5)	C(1)–O(7)	1.206(8)
Sn(3)–C(51)	2.108(12)	C(4)–O(11)	1.442(11)
Sn(3)–O(1)	2.148(3)	C(3)–O(9)	1.223(8)
Sn(3)–C(61)	2.132(6)	C(2)–O(10)	1.438(12)
Sn(3)–O(2)	2.151(3)	C(1)–O(6)	1.270(8)
Sn(3)–O(4)	2.056(4)		
Bond angles			
O(1)–Sn(1)–C(11)	110.7(2)	O(4)–Sn(4)–C(81)	94.24(19)
O(1)–Sn(1)–C(21)	123.4(5)	O(1)–Sn(4)–C(71)	116.3(3)
C(11)–Sn(1)–C(21)	125.9(5)	O(4)–Sn(4)–C(71)	103.7(2)
O(1)–Sn(1)–O(3)	74.58(15)	C(81)–Sn(4)–C(71)	123.0(3)
C(11)–Sn(1)–O(3)	96.0(3)	O(1)–Sn(4)–O(3)	74.20(15)
C(21)–Sn(1)–O(3)	96.0(6)	O(4)–Sn(4)–O(3)	148.32(16)
O(1)–Sn(1)–O(6)	81.86(15)	C(81)–Sn(4)–O(3)	93.6(2)
C(11)–Sn(1)–O(6)	96.6(3)	C(71)–Sn(4)–O(3)	97.4(2)
C(21)–Sn(1)–O(6)	93.1(6)	O(2)–Sn(5)–C(101)	121.5(3)
O(3)–Sn(1)–O(6)	155.99(16)	O(2)–Sn(5)–C(91)	115.4(3)
O(2)–Sn(2)–C(41)	119.8(5)	C(101)–Sn(5)–C(91)	123.1(4)
O(2)–Sn(2)–C(31)	107.7(3)	O(2)–Sn(5)–O(4)	75.22(14)
C(41)–Sn(2)–C(31)	132.4(6)	C(101)–Sn(5)–O(4)	97.3(2)
O(2)–Sn(2)–O(5)	74.57(16)	C(91)–Sn(5)–O(4)	99.2(2)
C(41)–Sn(2)–O(5)	98.2(6)	O(2)–Sn(5)–O(5)	74.00(16)
C(31)–Sn(2)–O(5)	91.5(3)	C(101)–Sn(5)–O(5)	97.8(2)
O(2)–Sn(2)–O(8)	81.11(16)	C(91)–Sn(5)–O(5)	94.7(3)
C(41)–Sn(2)–O(8)	94.5(7)	O(4)–Sn(5)–O(5)	149.21(17)
C(31)–Sn(2)–O(8)	95.2(3)	O(7)–C(1)–O(6)	125.1(7)
O(5)–Sn(2)–O(8)	155.67(16)	O(8)–C(3)–O(9)	124.7(7)
O(4)–Sn(3)–C(51)	114.6(5)	Sn(1)–O(1)–Sn(4)	110.36(16)
O(4)–Sn(3)–C(61)	117.4(2)	Sn(1)–O(1)–Sn(3)	143.04(19)
C(51)–Sn(3)–C(61)	128.0(5)	Sn(4)–O(1)–Sn(3)	104.67(14)
O(4)–Sn(3)–O(1)	74.53(13)	Sn(2)–O(2)–Sn(5)	110.46(17)
C(51)–Sn(3)–O(1)	97.7(5)	Sn(2)–O(2)–Sn(3)	144.1(2)
C(61)–Sn(3)–O(1)	95.18(19)	Sn(5)–O(2)–Sn(3)	105.11(15)
O(4)–Sn(3)–O(2)	74.26(14)	Sn(4)–O(3)–Sn(1)	100.85(16)
C(51)–Sn(3)–O(2)	97.9(4)	Sn(3)–O(4)–Sn(4)	105.35(15)
C(61)–Sn(3)–O(2)	96.4(2)	Sn(3)–O(4)–Sn(5)	105.38(15)
O(1)–Sn(3)–O(2)	148.64(15)	Sn(4)–O(4)–Sn(5)	148.6(2)
O(1)–Sn(4)–O(4)	75.36(14)	Sn(5)–O(5)–Sn(2)	100.59(17)
O(1)–Sn(4)–C(81)	120.5(2)		

monodentate coordination mode via Sn(1)–O(6) and Sn(2)–O(8) bonds with bond lengths 2.210(4) and 2.185(5) Å respectively. Although, distances Sn(1)–O(7) (3.062 Å) and Sn(2)–O(9) (3.108 Å) are longer than Sn–O covalent bond length but are much shorter than the sum of the van der Waals radii of tin and oxygen (3.7 Å) [33]. Therefore, the oxygen atoms O(7) and O(9) are involved in a weak interaction with tin [34,35]. The ring is an irregular macrocycle resembling almost a rectangle (Fig. 2) with the probable width 14.3 Å × 4.4 Å. The plane of the "ladder" cluster is almost perpendicular to the big conjugated rigid plane of ligand H_2L with the dihedral angle of 83° (see the side view of **1** in Fig. 2). Besides the bonds mentioned above, intermolecular hydrogen bonds O(5)–H(2)···O(9) (1.870 Å) and O(3)–H(1)···O(7) (2.019 Å) help complex **1** to form a kind of intermolecular 30-membered irregular ring (Fig. 3). And complex **1** is connected with each other forming a 2D-network through these interactions.

3.4. Anti-tumor activity

The results of cytostatic activity are listed in Table 3. IC_{50} values of the complex **1** are expressed in μM and compared with those of cisplatin. Complex **1** shows higher activities than *n*-Bu_2SnO in vitro antitumor activity in HeLa cell line. At concentrations of 10 μg/L, the results proved that complex **1** provides 91.2% growth inhibition, and the IC_{50} is 1.4 μg/mL. Complex **1** presents lower IC_{50} values than that of *n*-Bu_2SnO ($IC_{50} = 1.6$) and cisplatin ($IC_{50} = 3.50$) [36], which indicates its high activity against the tumoral cell line than *n*-Bu_2SnO and cisplatin. Based on these preliminary results, it can be figured out that activity of this complex **1** would be significant against antitumor effects.

3.5. Fluorescence spectra

The luminescent properties of solid **1** and free ligand H_2L have been tested with a 150 W xenon lamp as the excitation source at room temperature and the fluorescence emission spectra of them are illustrated in Fig. 4. The emission peak of the free ligand H_2L is at about 378 nm with the excitation peak at 340 nm, which is generally caused by $S_1 \rightarrow S_0$ transition. On complexation of the ligand with the Sn (IV) atom, complex **1** was red-shifted to 419 nm ($\lambda_{ex} = 320$ nm). The red-shift might be owing to the complexation of the ligand H_2L with the organooxotin cluster, which increases the conformational rigidity of the complex **1** and reduces the non-radiative decay of LMCT (Figs. 5 and 6).

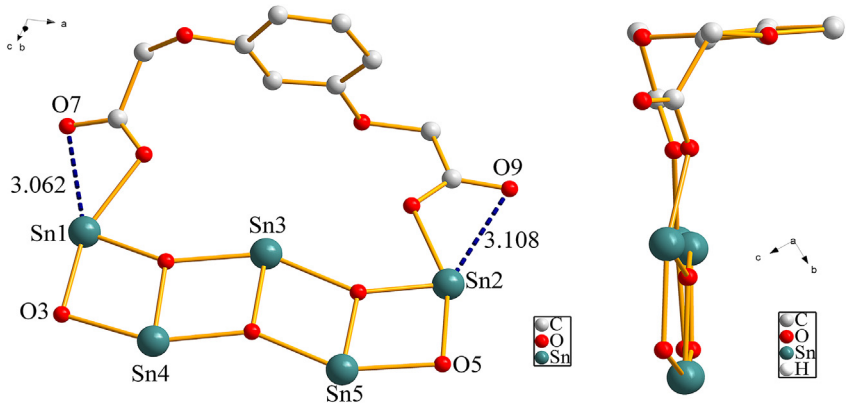

Fig. 2. The front and side views of complex **1**, the butyl groups are omitted for clarity.

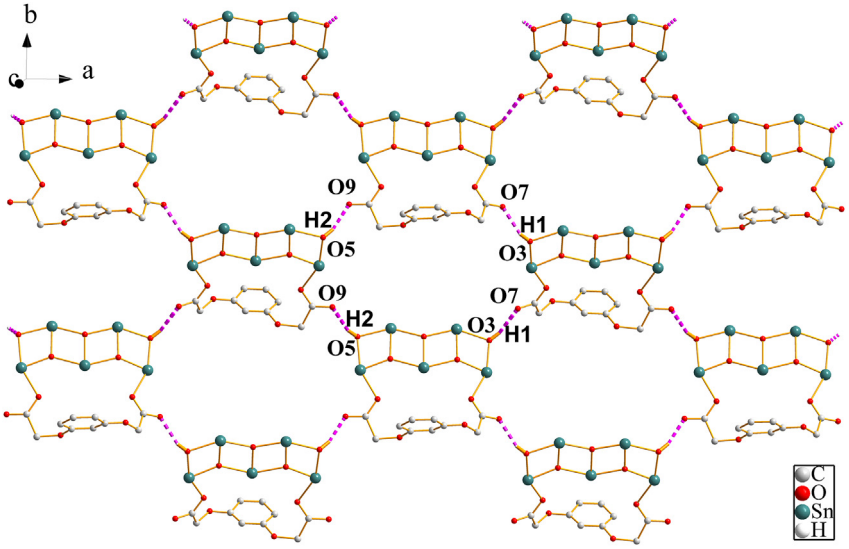

Fig. 3. Two dimensional molecular assembly of complex **1** formed by intermolecular C–H···O interactions, the butyl groups are omitted for clarity.

Table 3
In vitro antitumor activities of *n*-Bu_2SnO and complex **1** against Hela cell.

Compound	Dose (μg/mL)	Anticancer activity (%)	IC_{50} (μg/mL)
n-Bu_2SnO	0.1	1.1 ± 7.1	
	0.3	18.5 ± 3.3	
	1	29.8 ± 3.0	
	3	65.4 ± 1.5	
	10	88.1 ± 0.1	1.6
Complex **1**	0.1	1.6 ± 6.5	
	0.3	20.1 ± 3.4	
	1	32.3 ± 2.7	
	3	67.9 ± 1.2	
	10	91.2 ± 0.1	1.4

4. Conclusion

In conclusion, this paper describes the synthesis, characterization and antitumor activity of a novel macrocyclic organotin carboxylate containing one penta-nuclear four-fold-ladder organooxotin unit. Complex **1** shows fluorescence activity and the result of antitumor study is excellent. This study will be helpful in exploring various structures of organotin carboxylate and designing novel biological metal-based drugs.

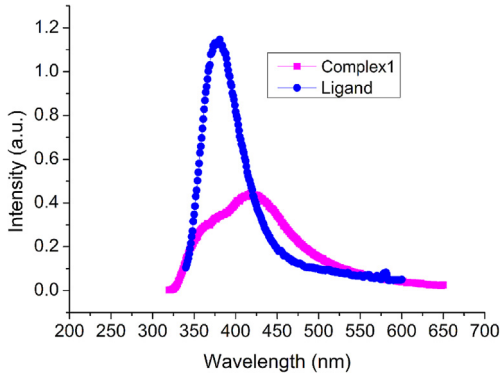

Fig. 4. Fluorescence emission spectra of ligand and **1**.

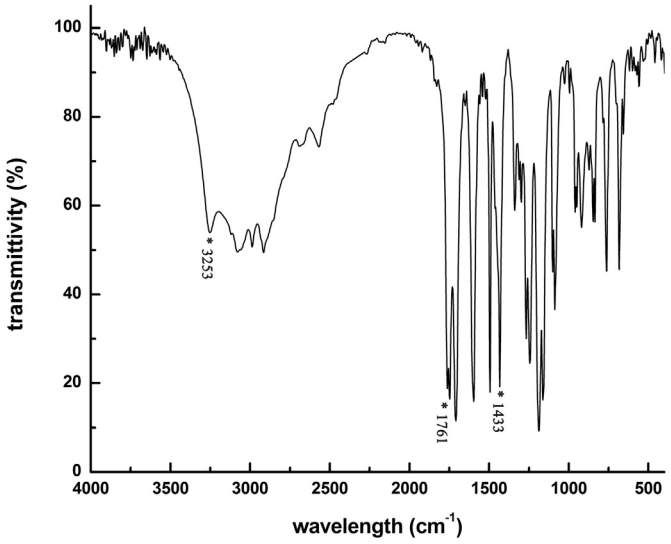

Fig. 5. IR spectrum of ligand.

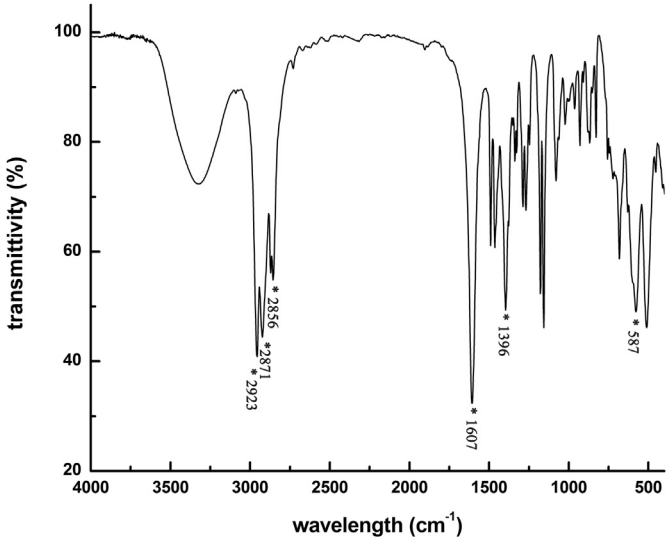

Fig. 6. IR spectrum of **1**.

Acknowledgments

We acknowledged the Science and technology department of Jilin province, China (no. 20120440 and 20130206109SF).

Appendix A. Supplementary material

CCDC 971881 contains the supplementary crystallographic data for this paper. These data can be obtained free of charge from The Cambridge Crystallographic Data Centre via www.ccdc.cam.ac.uk/data_request/cif.

References

[1] A.G. Davies, Organotin Chemistry, VCH, Weinheim, Germany, 1997.
[2] P.J. Smith, Chemistry of Tin, Blackie Academic & Professional, London, 1998.
[3] M.A. Champ, P.F. Seligman, Organotin. Environmental Fate and Effects, Chapman & Hall, London, 1996.
[4] M. Gielen, Appl. Organomet. Chem. 16 (2002) 481.
[5] S.J. Blunden, P.A. Cusack, R. Hill, Industrial Uses of Tin Chemicals, Royal Society of Chemistry, London, 1985.
[6] A.J. Crowe, in: M. Gielen (Ed.), Metal-based Drugs, vol. 1, Freund Publishing House, London, 1989, pp. 103–149.
[7] E.R.T. Tiekink, Trends Organomet. Chem. 1 (1994) 71.
[8] R.R. Holmes, Acc. Chem. Res. 22 (1989) 190.
[9] V. Chandrasekhar, S. Nagendran, V. Baskar, Coord. Chem. Rev. 235 (2002) 1.
[10] K.C. Molloy, T.G. Purcell, E. Hahn, H. Schumann, J.J. Zuckerman, Organometallics 5 (1986) 85.
[11] K.C. Molloy, K. Quill, I.W. Nowell, J. Chem. Soc. Dalton Trans. 12 (1987) 101.
[12] J.A. Zubita, J.J. Zuckerman, Inorg. Chem. 24 (1987) 251.
[13] G.K. Sandhu, R. Gupta, S.S. Sandhu, R.V. Parish, Polyhedron 4 (1985) 81.
[14] G.K. Sandhu, R. Gupta, S.S. Sandhu, R.V. Parish, K. Brown, J. Organomet. Chem. 279 (1985) 373.
[15] T.P. Lochhart, F. Davidson, Organometallics 6 (1987) 2471.
[16] I.W. Nowell, J.S. Brooks, G. Beech, R. Hill, J. Organomet. Chem. 244 (1983) 119.
[17] C.S. Parulekar, V.K. Jain, T.K. Das, A.R. Gupta, B.F. Hoskins, E.R.T. Tiekink, J. Organomet. Chem. 372 (1989) 193.
[18] J. Beckmann, D. Dakternieks, A. Duthie, F.S. Kuan, K. Jurkschat, M. Schürmann, E.R.T. Tiekink, New J. Chem. 28 (2004) 1268–1276.
[19] X. Xiao, D. Du, M. Tian, X. Han, J. Liang, D. Zhu, L. Xu, J. Organomet. Chem. 715 (2012) 54.
[20] D. Du, Z. Jiang, C. Liu, A.M. Sakho, D. Zhu, L. Xu, J. Organomet. Chem. 696 (2011) 2549.
[21] G. Zheng, J. Ma, J. Yang, Y. Li, X. Hao, Chem. Eur. J. 10 (2004) 3761.
[22] X. Xiao, K. Shao, L. Yan, Z. Mei, D. Zhu, L. Xu, Dalton Trans. 42 (2013) 15387.
[23] G.M. Sheldrick, SADABS. Program for Empirical Absorption Correction of Area Detector Data, University of Göttingen, Germany, 1996.
[24] G.M. Sheldrick, SHELXS-97, A Program for Automatic Solution of Crystal Structure, University of Göttingen, Germany, 1997.
[25] G.M. Sheldrick, SHELXL-97, A Program for Crystal Structure Refinement, University of Göttingen, Germany, 1997.
[26] L.J. Farrugia, WINGX, A Windows-based Program for Crystal Structure Analysis, University of Glasgow, Glasgow, UK, 1988.
[27] A. Varvaresou, K. Iakovou, Anticancer Res. 25 (2005) 2253.
[28] D. Kovala-Demertzi, N. Kourkoumelis, A. Koutsodimou, A. Moukarika, E. Horn, E.R.T. Tiekink, J. Organomet. Chem. 620 (2001) 194.
[29] K. Nakamoto, Infrared and Raman Spectra of Inorganic and Coordination Compounds, fourth ed., Wiley, New York, 1980.
[30] C. Ma, Q. Jiang, R. Zhang, D. Wang, Dalton Trans. 15 (2003) 2975.
[31] C. Ma, J. Sun, Dalton Trans. 15 (2004) 1785.
[32] M. Mehring, G. Gabriele, S. Hadjikakou, M. Schürmann, D. Dakternieks, K. Jurkschat, Chem. Commun. 8 (2002) 834.
[33] A. Bondi, J. Phys. Chem. 68 (1964) 441.
[34] A.R. Forrester, S.J. Garden, R.A. Howie, J.L. Wardell, J. Chem. Soc. Dalton Trans. 3 (1992) 2615.
[35] X. Xiao, X. Han, Z. Mei, D. Zhu, K. Shao, J. Liang, M. Tian, L. Xu, J. Organomet. Chem. 28 (2013) 729.
[36] G.N. Kaluđeroviæ, V.M. Đinoviæ, Z.D. Juraniæ, T.P. Stanojkoviæ, T.J. Sabo, J. Inorg. Biochem. 99 (2005) 488.